*Geophys. J. Int.* (2000) **141,** 595–604

# Numerical simulation of seismic waves using a discrete particle scheme

Aoife Toomey and Christopher J. Bean
*Department of Geology, University College Dublin, Belfield, Dublin* 4, *Ireland*

Accepted 1999 December 3. Received 1999 December 3; in original form 1999 February 1

## SUMMARY

A particle-based model for the simulation of wave propagation is presented. The model is based on solid-state physics principles and considers a piece of rock to be a Hookean material composed of discrete particles representing fundamental intact rock units. These particles interact at their contact points and experience reversible elastic forces proportional to their displacement from equilibrium. Particles are followed through space by numerically solving their equations of motion. We demonstrate that a numerical implementation of this scheme is capable of modelling the propagation of elastic waves through heterogeneous isotropic media. The results obtained are compared with a high-order finite difference solution to the wave equation. The method is found to be accurate, and thus offers an alternative to traditional continuum-based wave simulators.

**Key words:** finite difference methods, heterogeneity, particle-based model, wave propagation.



## 1 INTRODUCTION

Analytical methods allow us to model a wide spectrum of processes in the Earth Sciences and have enjoyed considerable success in crustal deformation and wave propagation studies for many decades. It is well known that inherent shortcomings in these schemes make it necessary to oversimplify (smooth) the geology in order to render the differential equations possible to solve. This shortcoming has become all the more acute with the growing realization of the highly heterogeneous nature of geological materials (e.g. Frankel 1989; Turcotte 1992; Marsan & Bean 1999). In reality, geological media are discontinuous over a broad scale range, being composed of discrete grains, neighbour–neighbour structural features and containing both macroscopic and microscopic fractures. In an effort to capture the effects of severe heterogeneity, numerical methods for simulating wave propagation through the Earth's crust have become important tools in the field of seismology over the past two decades. The development of numerical schemes has enabled us to study wave propagation through complex media for which analytical solutions to the wave equation must be severely truncated. These methods have proved valuable as a way of comparing real data obtained during seismic exploration with synthetic data from numerical models. They have also provided insights into the study of processes such as the scattering of seismic waves during their passage through the crust.

The most popular scheme is the finite difference (FD) method, which solves the wave equation by replacing the partial derivatives in space and time by their finite difference approximations. The solutions include all transmitted and reflected waves, *P*-to-*SV* and *SV*-to-*P* conversions, diffractions and scattered waves (e.g. Frankel 1989). Other schemes such as the boundary element method (e.g. Pointer *et al.* 1998) can also be used. Despite this success, schemes based on continuum methods may fail to model important aspects of wave propagation such as possible fluid movement in heterogeneous pore spaces. Consequently they require rather than provide observations for crucial processes such as intrinsic wave attenuation.

We introduce a numerical method that approaches the wave propagation problem from the discrete perspective. This approach, termed a 'discrete particle scheme' (DPS), is based not on the wave equation, but on the underlying physics of wave propagation that occurs at the atomic scale. Due to the limitations imposed by current computational power it is not possible to simulate rocks at the atomic scale; however, we can employ a particle-based approach in which particles represent larger units of intact rock, whose size depends on the application of the model and the available computational power. The geological medium is now described by a large number of these interacting particles, which are free to move in space subject to the constraints imposed by bonds with other particles. Waves propagate through the discrete lattice due to the interactions occurring at the contacts between the particles. A simple force–displacement interaction between the particles implicitly includes all boundary conditions between zones with different material properties and is shown here to capture elastic wave propagation in accordance with continuum mechanics.

## 2 DISCRETE PARTICLE SCHEMES

The discrete approach to modelling rock mechanics derives from solid-state physics models of microscopic crystals (e.g. Hoover *et al.* 1974), in which the crystal is considered to be made up of a closely packed lattice of particles interacting with Hooke's law forces. Cundall & Strack (1979) used a similar approach to model rock mechanics problems using the 'distinct element method', a numerical scheme in which particles representing blocks of rock interact through both radial and shear forces. The distinct element method has since been used extensively to model a diverse range of processes from rock fracture and mining and engineering applications to tectonic processes (Saltzer & Pollard 1992) and particulate mechanics (Williams *et al.* 1994). Other related methods include the 'lattice solid model' (Mora & Place 1993, 1994, 1998; Donze *et al.* 1994), which has been used to study earthquake dynamics. We now use these principles to investigate the propagation of elastic waves through a 2-D lattice of interacting particles. The model is composed of circular particles representing blocks of rock, arranged in a closely packed isotropic hexagonal configuration (Fig. 1). We chose this configuration as it resembles real rocks more closely than the more loosely packed cubic lattice. Each particle interacts radially with each of its six neighbours at the contact points, and the particles undergo displacement as a response to externally applied forces. We apply an external force in the form of a seismic source and examine the reaction of the medium to determine whether seismic waves propagate through the lattice in accordance with wave theory.

### 2.1 Lattice structure and properties

In the current 2-D scheme the particles are frictionless circular discs of area density $\rho$, separated by a distance $r_0$, the equilibrium particle spacing. Neighbouring particles are bonded together by virtual springs of stiffness $K$ which resist any displacement of particles from their equilibrium spacing. The particle properties determine the spring stiffnesses. The macroscopic properties of the medium are determined by the particle area density, equilibrium spacing and bond stiffnesses. Hoover *et al.* (1974) calculated Lamé's constants for a closely packed isotropic hexagonal lattice,

$$\lambda = \mu = \frac{K\sqrt{3}}{4}\,. \tag{1}$$

The area density per particle is

$$\rho = \frac{2m}{\sqrt{3}r_0^2}\,, \tag{2}$$

where $m$ is the particle mass. This leads to compressional and shear wave velocities of

$$V_p = r_0\sqrt{\frac{9K}{8m}}, \tag{3}$$

$$V_s = r_0\sqrt{\frac{3K}{8m}}. \tag{4}$$

The $P$-to-$S$-wave ratio for a hexagonal lattice is thus fixed at 1.73 and Poisson's ratio is 0.25. These values are typical of crustal rocks. A different lattice geometry would be required in order to change the $P$-to-$S$-wave ratio.

In the following simulations, each particle is assigned a density, diameter and $P$-wave velocity. The particle diameters determine the equilibrium spacing, $r_0$, between the particles. Eq. (2) gives the mass of each particle, and the stiffness of the bond joining two neighbouring particles is calculated from eq. (3). Neighbouring particles may have very different properties, in which case the bond stiffness is found by averaging the properties of the particles. The $S$-wave velocity is implicit.

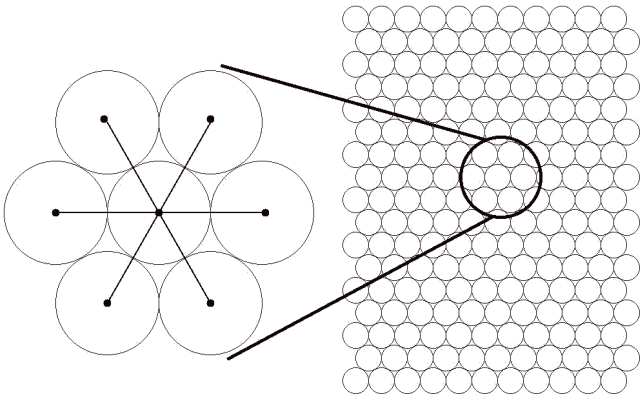

**Figure 1.** In discrete particle schemes the geological medium is considered to be made up of interacting particles whose meaning depends on the scale (e.g. blocks of rock, grains of sand). In these experiments we use a model in which the particles are arranged in a hexagonal geometry, with each particle bonded to its six nearest neighbours.

### 2.2 Particle interaction

Bonded particles interact at their contacts. This interaction is described by Hooke's law, which specifies the magnitude of the elastic force, $F$, acting between the two particles $i$ and $j$ as a result of compression or dilation of the spring joining them:

$$F_{(i,j)} = K_{(i,j)}(r_{(i,j)} - r_{0_{(i,j)}})\,, \tag{5}$$

where $r_{(i,j)}$ is the distance between the particle centres. This force can be resolved into components parallel to the horizontal and vertical axes,

$$F_{x_{(i,j)}} = F_{(i,j)}\cos\theta\,, \tag{6}$$

$$F_{z_{(i,j)}} = F_{(i,j)}\sin\theta\,, \tag{7}$$

where $\theta$ is the angle between the particles (Fig. 2). $\theta$ can be calculated from the horizontal ($x$) and vertical ($z$) distances between the particles as follows:

$$\cos\theta = \frac{x}{r}\,, \tag{8}$$

$$\sin\theta = \frac{z}{r}\,. \tag{9}$$

Since the positions of all particles in the simulation are known at all times, the forces acting at their contacts can be resolved. These forces are tensional if particles are stretched apart and compressional if particles are pushed together. The total force on any particle is the sum of the forces applied by each of its

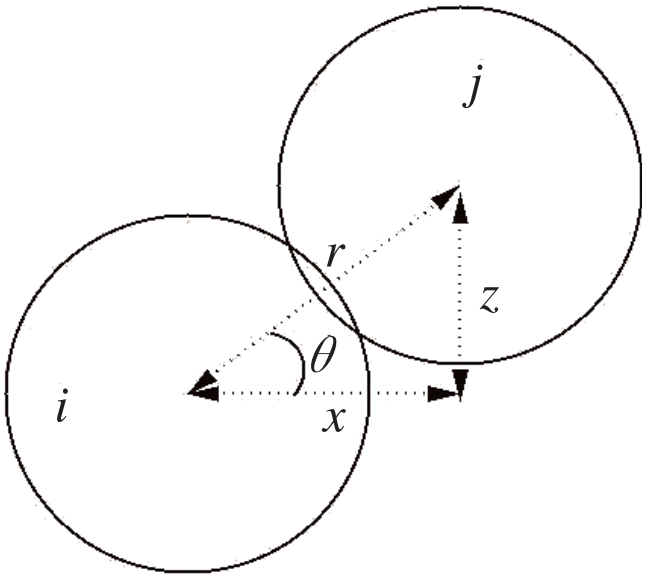


**Figure 2.** Particles interact at their contacts by means of reversible elastic forces. Two compressed particles experience a repulsive force proportional to the amount of overlap between them and the stiffness of the bond joining them. The force on any particle is the sum of the forces applied by each of its neighbours.

$N=6$ neighbours:

$$F_{x_i}=\sum_{j}^{N} F_{x_{(i,j)}}\,, \tag{10}$$

$$F_{z_i}=\sum_{j}^{N} F_{z_{(i,j)}}\,. \tag{11}$$

The bonds between particles are analogous to, for example, the interatomic potential, or at a much larger scale, the cement which bonds grains of sand together. Although Hooke's law describes a completely elastic system, the interaction rule can be altered to accommodate different rheologies. Since particle interactions are radial only, rotation of the particles is not considered.

The particles obey Newtonian dynamics, allowing their accelerations at the current time step to be found:

$$x_i''=\frac{F_{x_i}}{m}\,, \tag{12}$$

$$z_i''=\frac{F_{z_i}}{m}\,. \tag{13}$$

### 2.3 Numerical integration

Particle velocities and positions are extrapolated to the next time step using the velocity–Verlet numerical integration scheme (Allen & Tildesley 1987). This is a second-order finite difference approximation to the equations of motion. The accelerations are integrated first to give the current velocities,

$$x_i'(t)=x_i'(t-\Delta t)+\Delta t\,\frac{x_i''(t-\Delta t)+x_i''(t)}{2}\,, \tag{14}$$

$$z_i'(t)=z_i'(t-\Delta t)+\Delta t\,\frac{z_i''(t-\Delta t)+z_i''(t)}{2}\,. \tag{15}$$

The current velocities are integrated to give the positions at the next time step,

$$x_i(t+\Delta t)=x_i(t)+\Delta t x_i'(t)+\frac{\Delta t^2}{2!}\,x_i''(t)\,, \tag{16}$$

$$z_i(t+\Delta t)=z_i(t)+\Delta t z_i'(t)+\frac{\Delta t^2}{2!}\,z_i''(t)\,. \tag{17}$$

This completes the update of particle positions to the next time step, and the new interaction forces may now be calculated.

### 2.4 Numerical stability

Disturbances propagate through the lattice by means of forces at the contacts between particles. Since each particle reacts only to forces applied by its neighbours, it is important that any disturbance propagating through the lattice can cross only one particle in a given direction per time step. The time step must therefore be balanced against the maximum speed of propagation through the model, i.e. the maximum compressional wave velocity. This gives rise to the following stability criterion:

$$\Delta t<\frac{r_{0_{\min}}}{V_{\mathrm{p}_{\max}}}\,\frac{\sqrt{3}}{2}\,, \tag{18}$$

where $r_{0_{\min}}$ is the minimum interparticle spacing in the lattice. A similar condition is used in finite difference solutions to the wave equation.

## 3 WAVE PROPAGATION

The majority of numerical experiments using particle-based schemes have focused on modelling quasi-static tectonic processes, or non-elastodynamic effects such as fracturing. In these simulations, dynamic wave propagation is artificially damped out of the model (Mora & Place 1993, 1994). To our knowledge only a small number of discrete particle experiments have concentrated on elastodynamic processes. An example is the investigation of acoustic emissions, which are produced when failure occurs in rocks subjected to stress (Hazzard *et al.* 1998). These experiments are of interest in the areas of earthquake dynamics and the mechanics of rock failure. They simulate the high-frequency oscillations of particles which occur after bonds have broken in the lattice owing to external forces.

Here we introduce a method which allows us to model wave propagation without bringing the model to failure and which does not employ artificial damping. An artificial source (Fig. 3) is input as a force on a particle on the lattice, in a manner analogous to the artificial explosive sources used in traditional wave simulations in controlled-source seismology. In this manner we are able to control the frequency and wavelength of the source, ensuring that no dispersion occurs (see Section 3.1). The results of these simulations must be compared to an analytical solution to the wave equation to judge their accuracy. We compare our results to those obtained using a high-order finite difference solution to the wave equation, which has already been demonstrated as accurate by comparison with analytical solutions (Igel 1993).

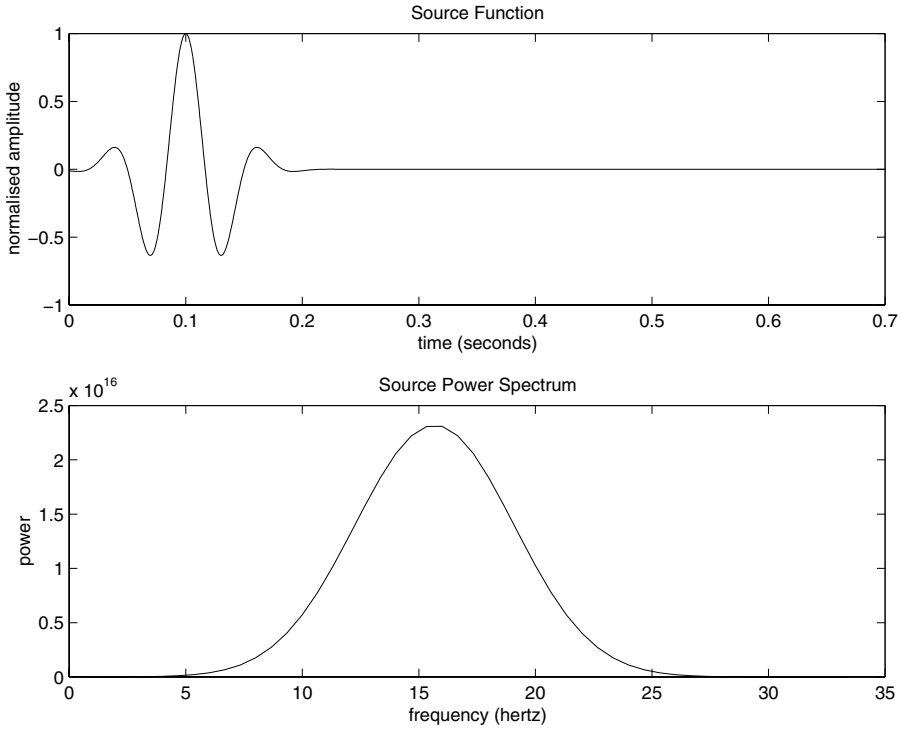


**Figure 3.** Wave propagation is initiated by inputting a source function with a central frequency of 16 Hz as a vertical force on the particle at the centre of the lattice.

### 3.1 Dispersion

Wave speeds are a function of wavelength in a discrete lattice. We have carried out an investigation of the dispersive properties of our model to see if they are in accordance with theoretical dispersion relations provided by solid-state physics (e.g. Young 1992).

In the case of a plane longitudinal wave propagating through a cubic lattice, the particles are displaced in the direction of propagation of the wave. All particles in a plane perpendicular to the wave move in unison, so we need consider only one row of particles, parallel to the direction of propagation (Fig. 4). The equilibrium position of each particle $j$ is $j$ times $r_0$. During wave propagation, each particle is displaced along the $x$ axis by a distance $x_j$. The force on particle $j$ is given by Hooke's law,

$$F_j = K(x_{j+1} - 2x_j + x_{j-1}), \tag{19}$$

and its acceleration is given by Newton's law,

$$F_j = m\frac{d^2x_j}{dt^2}. \tag{20}$$

If the wave travelling through the lattice has the wavefunction

$$\sin(\omega t - kx), \tag{21}$$

where $x$ is the equilibrium position of the $j$th particle and $k$ is the wavenumber ($2\pi/\lambda$), then the displacement of the $j$th particle due to the wave is

$$x_j(t) = \sin(\omega t - kjr_0) \tag{22}$$

and its acceleration is

$$\frac{d^2x_j}{dt^2} = -(\omega)^2 \sin(\omega t - kjr_0). \tag{23}$$

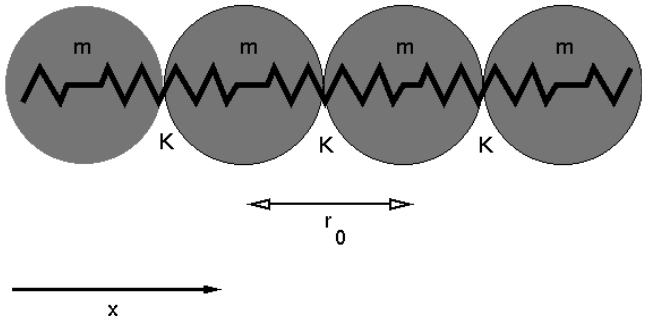


**Figure 4.** A portion of the 1-D lattice used to investigate dispersion.

Substituting these back into eqs (19) and (20) gives

$$\omega = 2\sqrt{\left(\frac{K}{m}\right)}\sin\left(\frac{kr_0}{2}\right). \tag{24}$$

This is an important result because it shows that $\omega$ is a function of $\sin(k)$ and thus the wave speed $\omega/k$ is also a function of $\sin(k)$, i.e. the wave is dispersive. Fig. 5 shows the relation between $\omega$ and $k$.

If the wavelength $\lambda$ is much larger than the lattice spacing $r_0$, then

$$\frac{1}{k} \gg r_0, \tag{25}$$

therefore

$$kr_0 \ll 1, \tag{26}$$

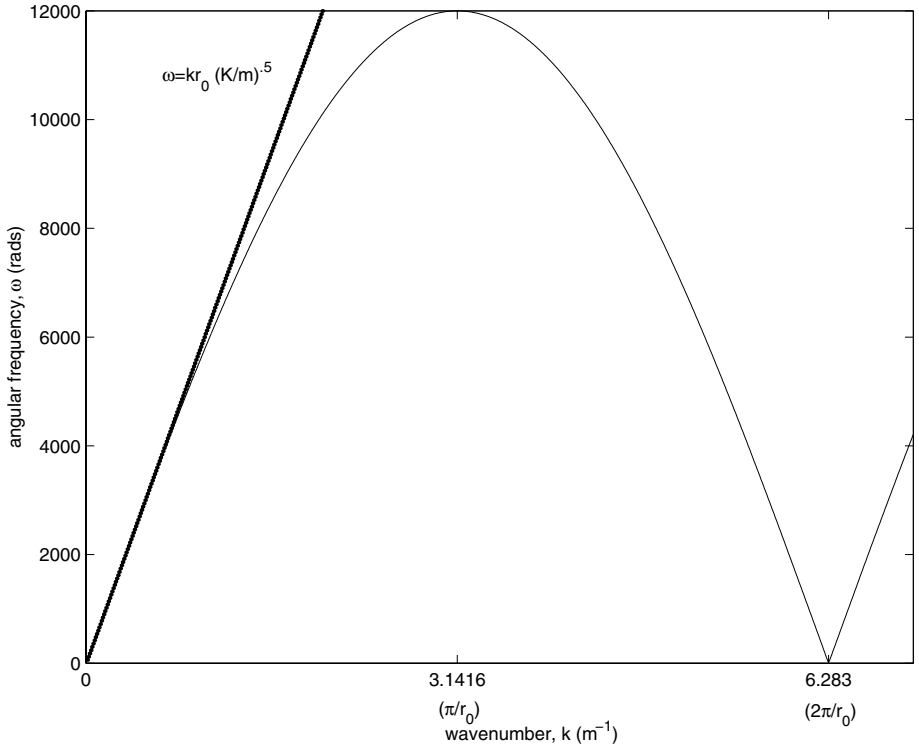


**Figure 5.** In a discrete lattice, the wave speed $\omega/k$ is not constant but varies with $k$, i.e. different frequencies propagate at different velocities. For small $k$ the curve is approximately linear and all frequencies propagate at approximately the same velocity, $r_0\sqrt{(K/m)}$.

so

$$\sin\left(\frac{kr_0}{2}\right) \approx \frac{kr_0}{2}\,. \tag{27}$$

In this case

$$\omega \approx 2\sqrt{\left(\frac{K}{m}\right)}\frac{kr_0}{2} \tag{28}$$

and thus the velocity in a 1-D lattice is

$$\frac{\omega}{k} \approx r_0\sqrt{\frac{K}{m}}. \tag{29}$$

Hence, when the wavelength is much larger than the lattice spacing, the dispersion becomes practically undetectable. This can be seen in Fig. 5—for small $k$ the curve is approximately linear. For shorter wavelengths the waves begin to 'see' the discrete nature of the lattice. For $\omega$ greater than $2\sqrt{K/m}$ there is no value of $k$ for which eq. (24) is satisfied. This is the maximum possible angular frequency of waves in the lattice.

We have examined the dispersive properties of a 1-D version of our model. A series of monochromatic sources, with a range of frequencies and the wavefunction given by eq. (21), were input as a displacement of one of the particles in the lattice. The resultant wavefield was then examined at a distance of 200 wavelengths from the source. The time taken for the wave to arrive at this location was used to calculate its velocity and wavelength. The results in Fig. 6 show that for seismic frequencies the lattice clearly obeys the theoretical dispersion relation. The number of particles required per seismic wavelength to eliminate dispersion depends on the size of the model—a wave which appears to be non-dispersive close to the source may be quite obviously dispersed a greater distance away. For our current implementation, 10 particles per seismic wavelength are sufficient to reduce dispersion to below a detectable level.

A similar criterion must be applied in finite difference solutions to the wave equation. However, many implementations of finite difference schemes use higher-order updates to the displacement field. Consequently, they are non-dispersive for much smaller wavelengths than our scheme. The finite difference solution used in this paper is eighth order in space and second order in time on a staggered grid and is non-dispersive for as few as four grid nodes per seismic wavelength (Igel 1993).

## 4 NUMERICAL EXPERIMENTS

We carried out the following experiments using the discrete particle scheme and compared the results to those obtained from finite difference wave simulations carried out using identical parameters. The following source function was used to generate a source with a central frequency of 16 Hz and a maximum frequency of 30 Hz (Fig. 3):

$$\text{source}(t) = \exp\left[-\frac{1}{2}\,(2f(t-200)\Delta t)^2\right]\cos 2\pi f(t-200)\Delta t\,. \tag{30}$$

The source was input as a force in the $z$ direction on the particle at the centre of the lattice. The displacements of individual particles at specified locations were then followed in time and snapshots of the displacement field over the entire model were recorded. Two different elastic models were used—a homogeneous model and a layered model. In each case the particle diameter in the DPS simulations and the grid spacing in the FD model were 10 m. Both models had a constant density

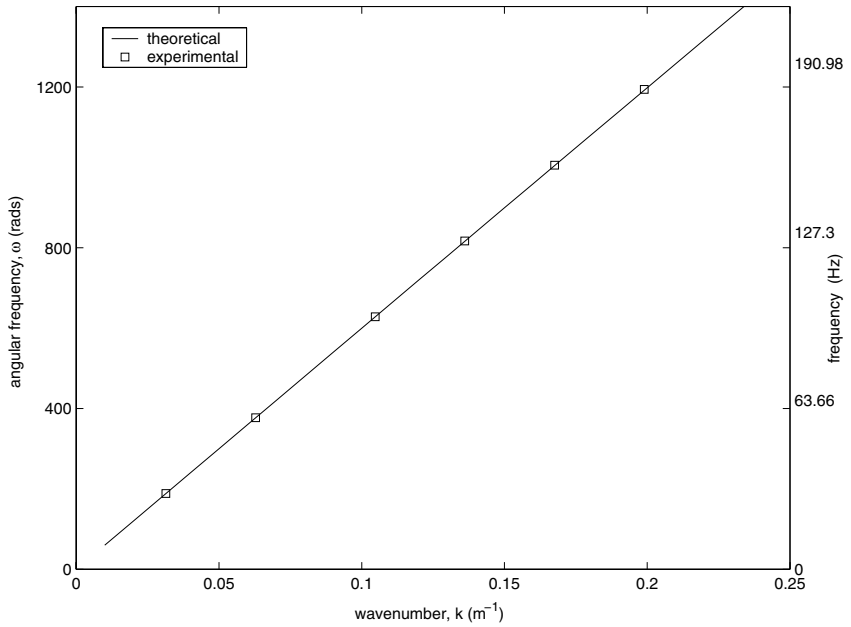


**Figure 6.** Experimental measurements of dispersion in a 1-D discrete particle lattice are in agreement with the theoretical dispersion relations provided by solid-state physics. The investigation was restricted to seismic frequencies, hence only a small portion of the theoretical curve is shown here.

of 2000 kg m$^{-2}$. We used a time step of $5 \times 10^{-4}$ s. Both numerical methods required the same order of computational expense.

### 4.1 Homogeneous model

We investigated wave propagation through a $6000 \times 6000$ m homogeneous model with a compressional wave velocity of 6000 m s$^{-1}$ and an *S*-wave velocity of 3464 m s$^{-1}$. The source was input at the centre of the lattice and synthetic seismic traces were collected along two horizontal profiles located at depths of 3000 and 4500 m.

Fig. 7 shows snapshots of the normalized displacement fields taken after 0.5 s. The results of the discrete particle simulation are shown in (a), and the finite difference results are shown in (b). The displacements have been normalized to facilitate

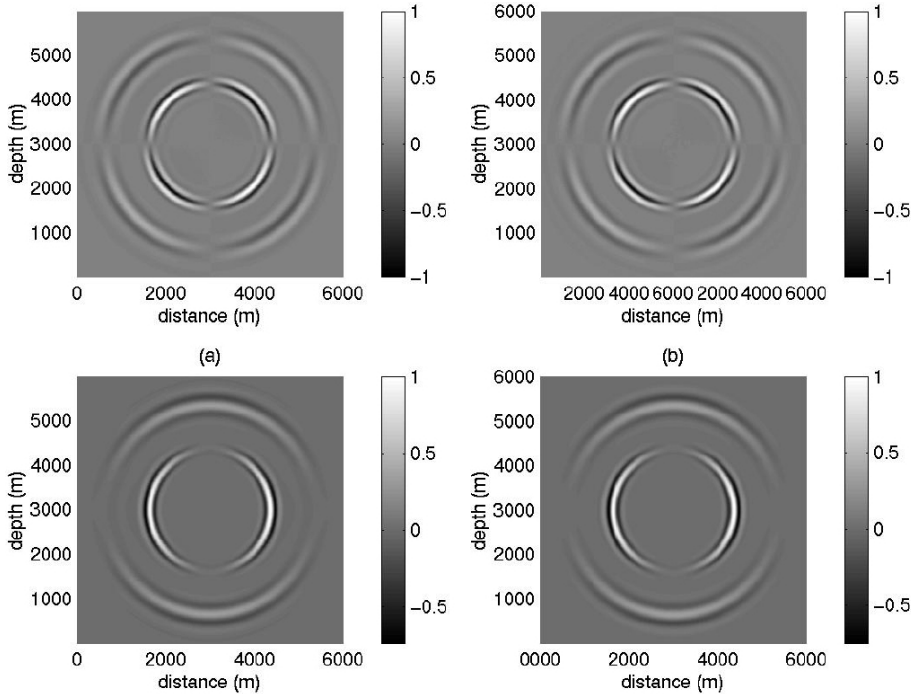


**Figure 7.** Snapshots of the normalized displacement field at time step 1000 (0.5 s), for a vertical source. Greyscale variations represent amplitude of displacement in the *x* (upper figures) and *z* (lower figures) directions. The *x* and *z* components of displacement in the discrete particle model (a) are compared to the *x* and *z* components in the finite difference model (b).

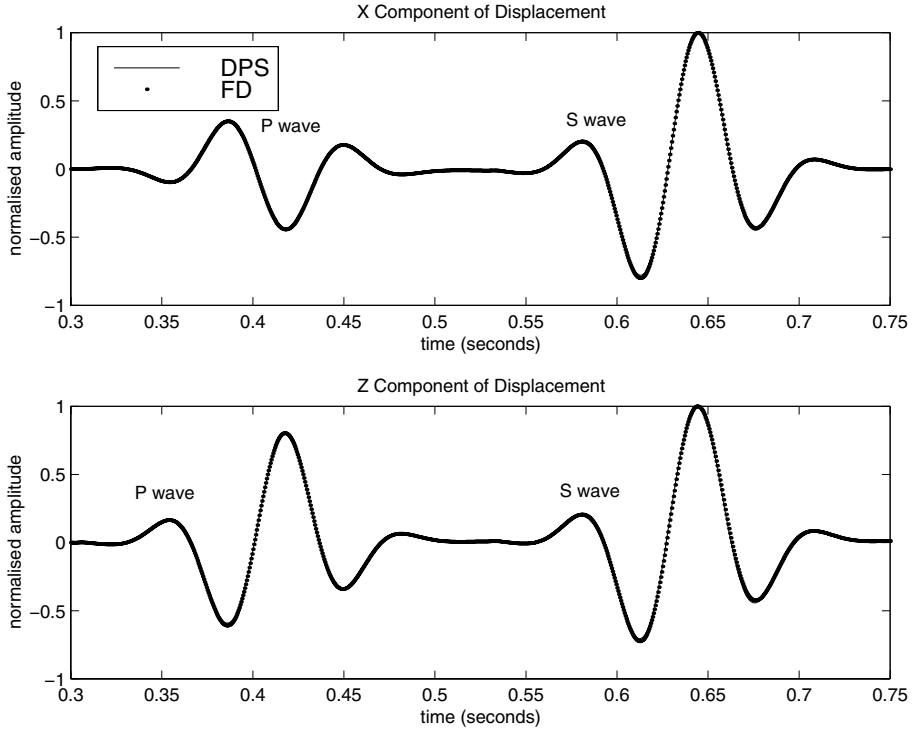


**Figure 8.** Normalized seismic traces showing the $x$ and $z$ components of displacement at a location 1860 m from the source in the upper-left quadrant of the model. Discrete-particle results (solid traces) are compared to finite difference results (dotted traces). These figures show the direct $P$-wave arrival followed by the direct $S$ wave.

direct comparison between the results. The $x$ components of displacement (upper figures) show $P$ waves travelling at a velocity of 6000 m s$^{-1}$ followed by the slower shear waves travelling at 3464 m s$^{-1}$. These velocities have been confirmed by measuring them from the synthetic seismic sections. The snapshots of the $z$ components of displacements show $P$ waves propagating in the direction of the source displacement (along the $z$ axis) and shear waves propagating at right angles to this, in the $x$ direction. The snapshots show very similar results, and are examined in greater detail in Fig. 8, in which we compare individual traces from a particle located in the upper left quadrant of the model, at a distance of 1860 m from the source. This distance represents approximately nine compressional wavelengths, and 16 shear wavelengths. Fig. 8 shows the normalized $x$ and $z$ components of displacement in the discrete particle scheme (solid traces) overlain by those of the finite difference simulation (dotted traces). The first arrivals are $P$ waves, followed by shear waves. The results are very similar.

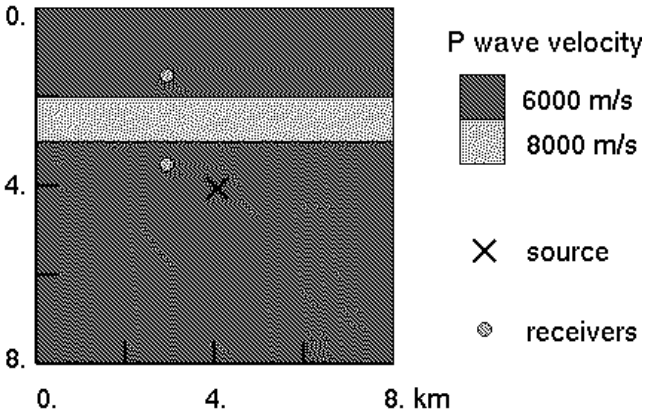


**Figure 9.** Geometry of the layered model used in the numerical experiment. The model is an $8 \times 8$ km isotropic elastic medium with a $P$-wave velocity of 6000 m s$^{-1}$ containing a thin layer of higher velocity (8000 m s$^{-1}$).

### 4.2 Layered model

The second model consisted of a $8000 \times 8000$ m grid of $P$-wave velocity 6000 m s$^{-1}$ and $S$-wave velocity 3464 m s$^{-1}$, containing a 1000-m-thick layer with a $P$-wave velocity of 8000 m s$^{-1}$ and an $S$-wave velocity of 4619 m s$^{-1}$. The high-velocity layer is located 1000 m from the source, as shown in Fig. 9. The source was input as before, and the reflected and transmitted wavefields were sampled at the locations marked in Fig. 9.

Fig. 10 shows snapshots of the normalized displacement field taken after 0.5 s. This shows the direct $P$ and $S$ waves propagating outwards from the source, $P$ and $S$ wave reflections and transmissions, $P$-to-$S$-wave conversions at the boundary between the two layers, and events from within the layer. The transmitted wavefield was sampled at a distance of 2773 m from the source, and was found to be very similar in the DPS and FD models (Fig. 11). The displacements due to the reflected wavefield (Fig. 12), sampled 1300 m from the source, are also very similar. Due to the different lattice geometries (hexagonal in DPS and square in FD) slight differences in the source, receiver and interface positions will occur. This can give rise to some of the observed differences in the recorded seismograms.

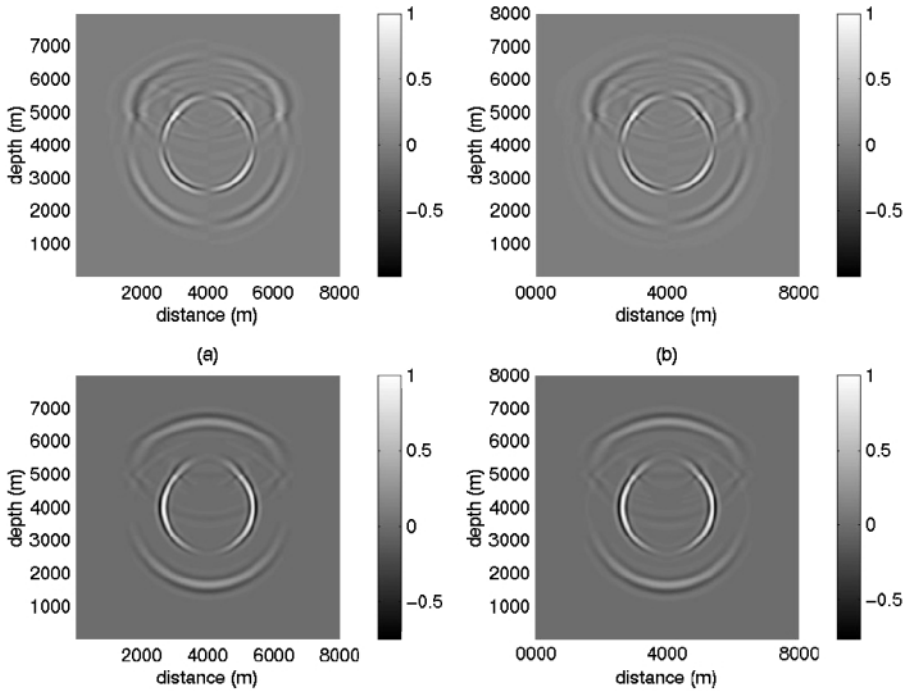


**Figure 10.** Snapshots of the normalized displacement field in the heterogeneous model at time step 1000, or 0.5 s, for a vertical source. Discrete particle results are shown in (a) while finite difference results are shown in (b). The upper figures show displacements in the $x$ direction and the lower ones show displacements in the $z$ direction.

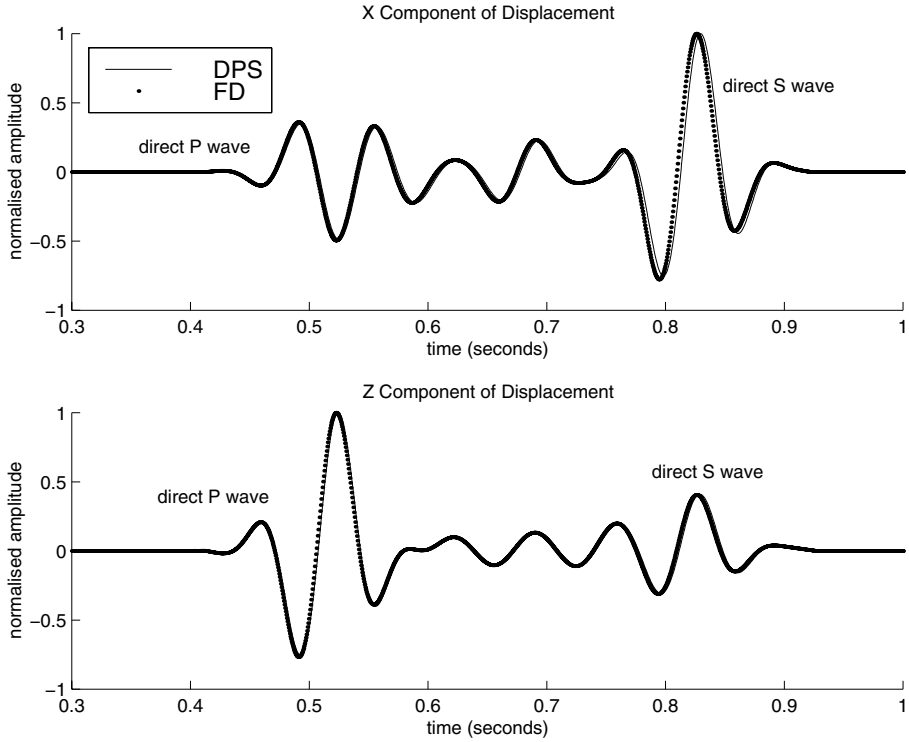


**Figure 11.** Normalized $x$ and $z$ components of displacement at a location 2773 m from the source. This shows the transmitted wavefield in the discrete particle model (solid trace) overlain by the displacements in the finite difference model (dotted trace). Edge effects have been suppressed.

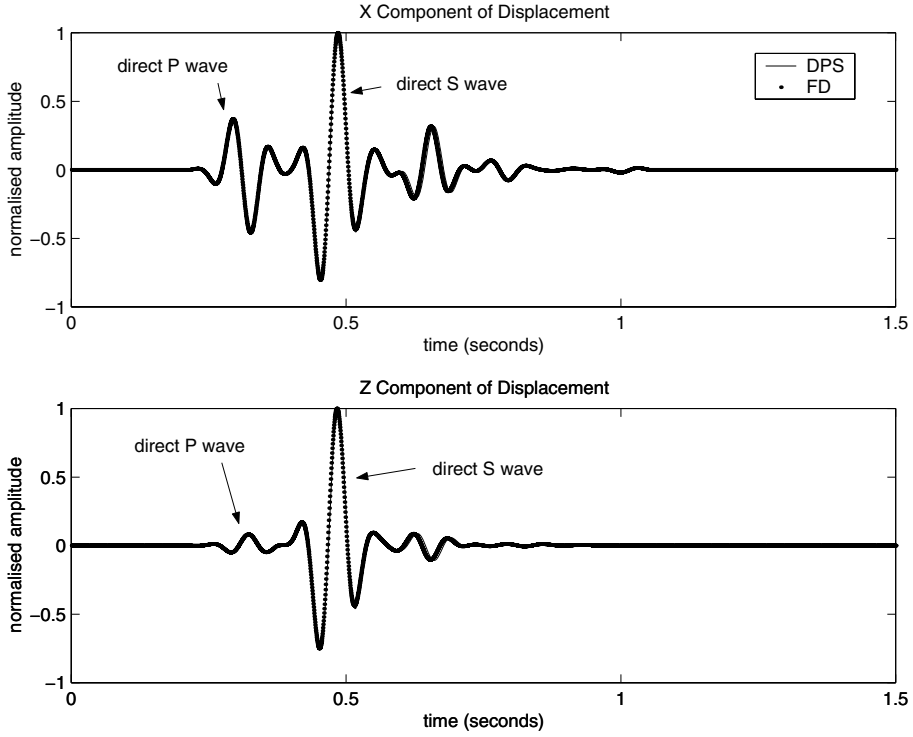


**Figure 12.** These traces are taken from a location 1300 m from the source. This shows the direct arrivals, reflections from the high-velocity layer, and events from within the layer. Edge effects have been suppressed.

## 5 CONCLUSIONS

Our results show that this implementation of a discrete particle scheme can be used to model elastic wave propagation in heterogeneous media with the same accuracy and the same order of computational expense as a high-order finite difference solution to the wave equation. The hexagonal lattice geometry used in this implementation leads to a Poisson's ratio fixed at 0.25. Investigations of wave propagation through heterogeneous media suggest that the method offers an alternative to wave simulators based on continuum physics. This opens up new avenues for numerical experiments involving more realistic random particle sizes, geometries and properties. Friction (Dobrin 1988), thermal diffusion (Leary 1995) and fluid squirting (Wulff & Burkhardt 1996) have been proposed as causes of wave attenuation. This method may provide an alternative way to investigate these phenomena numerically. For example, it may be possible to incorporate particle-based fluids residing in arbitrary heterogeneous porosity into wave simulations, using a similar scheme to that proposed in this work. It is hoped that this will provide a useful tool for investigating wave propagation in multiphase heterogeneous media.

## ACKNOWLEDGMENTS

The authors are grateful to Heiner Igel for the use of the finite difference wave simulation code used in these experiments. We thank Bertrand Maillot for detailed comments and Oona Scotti and Philippe Volant for discussions. Financial support from Enterprise Ireland is acknowledged.

## REFERENCES

Allen, M.P. & Tildesley, D.J., 1987. *Computer Simulations of Liquids,* Oxford University Press, New York.

Cundall, P.A. & Strack, O.D.L., 1979. A discrete numerical model for granular assemblies, *Geotechnique,* **29,** 47–65.

Dobrin, M.B., 1988. *Introduction to Geophysical Prospecting,* 4th edn, McGraw-Hill, New York.

Donze, F., Mora, P. & Magnier, S.A., 1994. Numerical simulation of faults and shear zones, *Geophys. J. Int.,* **116,** 46–52.

Frankel, A ., 1989. A review of numerical experiments on seismic wave scattering, *PAGEOPH,* **131,** 639–685.

Hazzard, J.F., Maxwell, S.C. & Young, R.P., 1998. Micromechanical modelling of acoustic emissions, in *Conference Proceedings—Eurrock 98 Conference on Rock Mechanics,* pp. 519–525, Trondheim, Norway.

Hoover, W.G., Ashurst, W.T. & Olness, R.J., 1974. Two-dimensional computer studies of crystal stability and fluid viscosity, *J. chem. Phys.,* **60,** 4043–4047.

Igel, H., 1993. Seismic modelling and inversion, *PhD thesis,* University of Paris 7, France.

Leary, P.C., 1995. The cause of frequency-dependent seismic absorption in crustal rock, *Geophys. J. Int.,* **122,** 143–151.

Marsan, D. & Bean, C.J., 1999. Multiscaling nature of sonic velocities and lithology in the upper crystalline crust: evidence from the KTB Main Borehole, *Geophys. Res. Lett.,* **26,** 275–278.

Mora, P. & Place, D., 1993. A lattice solid model for the nonlinear dynamics of earthquakes, *Int. J. mod. Phys. C,* **4,** 1059–1074.

Mora, P. & Place, D., 1994. Simulation of the frictional stick-slip instability, *PAGEOPH,* **143,** 61–87.

Mora, P. & Place, D., 1998. Numerical simulation of earthquake faults with gouge: toward a comprehensive explanation for the heat flow paradox, *J. geophys. Res.,* **103**(B9), 21 067–21 089.

Pointer, T., Liu, E. & Hudson, J.A., 1998. Numerical modelling of seismic waves scattered by hydrofractures: application of the indirect boundary element method, *Geophys. J. Int.,* **135,** 289–303.

Saltzer, S.D. & Pollard, D.D., 1992. Distinct element modelling of structures formed in sedimentary overburden by extensional reactivation of basement normal faults, *Tectonics,* **11,** 165–174.

Turcotte, D.L. 1992. *Fractals and Chaos in Geology and Geophysics,* Cambridge University Press, Cambridge.

Williams, J.R., Rege, N. & O'Connor, R., 1994. Particulate mechanics of manufacturing processes, in *Proc. IMM Summer Workshop Mechanics and Statistical Physics of Particulate Materials,* La Jolla, CA.

Wulff, A.M. & Burkhardt, H., 1996. The influence of local fluid flow and the microstructure on elastic and anelastic rock properties, *Surv. Geophys.,* **17,** 347–360.

Young, H.D., 1992. *University Physics,* Addison Wesley, Reading, MA.